

Observation of Nuclear Ferromagnetic Ordering in Silver at Negative Nanokelvin Temperatures

P. J. Hakonen, K. K. Nummila, R. T. Vuorinen, and O. V. Lounasmaa

Low Temperature Laboratory, Helsinki University of Technology, 02150 Espoo, Finland

(Received 15 October 1991)

The ferromagnetically ordered state in the nuclear spin system of silver has been reached at negative absolute temperatures by adiabatic nuclear demagnetization at entropies below $0.82\mathcal{R}\ln 2$. The ordering, caused by the antiferromagnetic Ruderman-Kittel interaction, was observed below -1.9 nK as a saturation of susceptibility close to -1 and as an increase of the NMR frequencies. Comparison with recent mean-field calculations by Viertiö and Oja suggests a domain configuration. The phase diagram of silver nuclei at $T < 0$ is outlined in the magnetic field versus entropy plane.

PACS numbers: 75.30.Kz, 75.90.+w

Nuclear magnetic ordering has been studied extensively at $T > 0$ in copper and silver. In these metals, competition between the dipolar force and the antiferromagnetic exchange interaction leads to interesting phase diagrams below the transition temperatures of 58 nK and 560 pK, respectively [1-3]. Fundamentally different behavior is expected when $T < 0$ [4,5].

At positive temperatures the distribution of spins among the Zeeman levels is given by the usual Boltzmann factor, $\exp(-\mu B/kT)$. Since the energy spectrum of nuclear spins is limited, a population inversion is possible, e.g., by reversing the magnetic field quickly in a time $t < \tau_2 = 10$ msec, so that the spins do not have a chance to redistribute themselves among the energy levels. This state of inverted spin populations can also be described by the Boltzmann distribution but with a negative absolute temperature. At $T < 0$, an isolated spin system has the highest possible Helmholtz free energy. In silver, which is dominated by an antiferromagnetic Ruderman-Kittel exchange interaction, this favors parallel alignment of the spins and, consequently, leads to a ferromagnetic ordering, which provides the state of maximum energy at $T < 0$.

In our earlier experiments on silver [6], a clear tendency to ferromagnetism was seen when the measured susceptibility data were fitted with the Curie-Weiss law, but the transition point was not reached. After vital improvements in our experimental techniques, we are finally able to report in this Letter the first observation of the ferromagnetically ordered nuclear spin state in a metal at $T < 0$. This ferromagnetic ordering, caused by an antiferromagnetic interaction, is a concrete example of the significance of spin temperatures. At $T > 0$, the very same interactions produce antiferromagnetic order.

The Hamiltonian in silver can be written in the form

$$H = H_{\text{dip}} + H_{\text{ex}} + H_Z \\ = H_{\text{dip}} - \sum_i J_{ij} \mathbf{I}_i \cdot \mathbf{I}_j - \hbar \mathbf{B} \cdot \sum_i \gamma_i \mathbf{I}_i, \quad (1)$$

where \mathbf{B} is the external magnetic field appearing in the Zeeman term H_Z . The dominating spin-spin energy is the nearest-neighbor exchange interaction H_{ex} , whose strength can be estimated from earlier NMR experiments

[7,8] which yield $J/\hbar = -26.5$ Hz for the exchange integral; the dipolar energy H_{dip} is smaller roughly by a factor of 3. Natural silver is composed of two isotopes ^{107}Ag and ^{109}Ag ; both have spin $I = \frac{1}{2}$. Their gyromagnetic ratios γ are sufficiently close so that, at low fields, the NMR lines merge.

Our silver sample, of nominal purity 99.99+%, consisted of 48 polycrystalline foils with dimensions $8 \times 0.025 \times 65$ mm³, oriented along the x , y , and z directions, respectively. The assembly of the specimen is described in Ref. [9]. In order to facilitate the production of negative temperatures by the rapid field reversal, the new coil set-up and the radiation shields were carefully prepared to prevent eddy currents which must have been the main problem during our previous, less successful experiments [6]. Two saddle-shaped static field coils of lengths 60 and 65 mm and one 70 mm long solenoid for B_z , all wound of 50- μm multifilamentary NbTi superconducting wire, were located on a coil former (diameter of 14 mm) inside the brass radiation shield (diameter of 16.5 mm) which had four cuts symmetrically along its length. The astatically wound pickup coil was oriented parallel to the z axis.

The experiments were carried out in our cascade nuclear demagnetization cryostat [10]. Achieving a high polarization in silver is a slow process: The spin-lattice relaxation time $\tau_1 = 14$ h at 200 μK . Details of the cooling process and experimental techniques are described in Ref. [9]. However, the demagnetization sequence was modified: We employed degaussing of the second stage magnet ($+7.4$ T \rightarrow -0.1 T \rightarrow $+0.02$ T \rightarrow 0) to guarantee proper operation of the SQUID measurement system, susceptible to vibrational noise in the presence of a small remanent field. Fortunately, this procedure did not substantially decrease the largest initial polarization, $p = 0.85$, achieved in these experiments. Measurements of the longitudinal adiabatic susceptibility were employed to determine the remanent field which varied between 0 and 5 μT .

NMR spectra, measured at 200 μT , were used to calculate the polarization from the equation [4] $p = A \int \chi''(f) df$; the proportionality constant A was calibrated against the Pt-NMR temperature scale around 1

mK [9]. We also employed the frequency shifts of the NMR lines, with the static field along the x and y axes, to determine the ratio of the demagnetization factors $D_x:D_y \cong 1:3$ for our sample; on the basis of this we estimate $D_x = 0.25$, $D_y = 0.75$, and $D_z = 0$.

The solenoidal magnetic field B_z employed in the rapid field reversal was typically $400 \mu\text{T}$. Our best inversion efficiency, 90%, was reached for small initial polarizations on the order of $p = 0.30$. At high polarizations, the results varied irregularly. Despite many efforts by changing the speed (0.5–5 msec), symmetry, and magnitude of the field flip, the optimum inversion efficiency was only 60%–75% at $p = 0.85$. Therefore, polarizations at $T < 0$ were limited to $p \cong -0.65$. In copper, production of negative temperatures has not succeeded owing to the short $\tau_2 = 150 \mu\text{sec}$.

Figure 1 displays NMR line shapes measured in zero field. Instead of absorption, as at $T > 0$, the system is emitting energy when $T < 0$. The emission maximum shifts towards higher frequencies with increasing polarization. The solid curves are fits of Lorentzian line shapes to the measured spectra, with the negative frequency side included; the least-squares minimization was done for the emission and dispersion curves, simultaneously. The static susceptibility was obtained from the fits by using the Kramers-Krönig relation $\chi'(0) = (2/\pi) \times \int_0^\infty (\chi''/f) df$; the upper limit of integration was set to 200 Hz. The absolute value of the susceptibility was calibrated in the paramagnetic state by using the equation [9] $1/\chi'(0) = B/\mu_0 p M_{\text{sat}} + D_z - D_y$, where $\mu_0 M_{\text{sat}} = 45.1 \mu\text{T}$ is the field corresponding to saturation magnetization.

Figure 2 displays the static susceptibility $\chi = \chi'(0)$, in-

tegrated from the Kramers-Krönig relation, as a function of polarization in zero field and at four different values of B_y ; at $5 \mu\text{T}$, data obtained in the parallel field B_z are also shown. At zero field and at $5 \mu\text{T}$, there is first a monotonous increase of $\chi'(0)$ with p , which then saturates between $p = -0.4$ and -0.5 . According to studies on dielectric materials [4] and the mean-field calculations to be discussed below, this behavior is caused by ferromagnetic ordering; the susceptibility is governed by dipolar interaction through the formation of ferromagnetic domains which, in the ideal case, leads to $\chi = -1$ for our sample.

In zero field and at small polarizations the susceptibility of silver is of the form $1/\chi = 1/\chi_0 + R + L - D_z$, where $\chi_0 = 1.30p$ is the Curie-law susceptibility of the noninteracting spin system (see Ref. [9]) and the Lorentz factor $L = \frac{1}{3}$. The uppermost curve in Fig. 2 is the best fit of points with $|p| < 0.45$ by this equation, using $R = -1.1$ which differs quite a lot from the value $R = -2.5 \pm 0.5$ obtained from the NMR experiments [8]. This indicates that substantial deviation from the mean-field behavior takes place already at intermediate polarizations. Within the scatter of the measured data, the same curve fits the experimental results at $B = 0$ and at $B = 5 \mu\text{T}$. As is typical for dipolar ferromagnetism [4], our data do not saturate completely even when the polarization is high but, nevertheless, we have described the results for $|p| > 0.55$ approximately by a constant line, $\chi = \chi_{\text{sat}} = -1.05$.

We identify the crossing of the two lines in Fig. 2 as the transition point to the ferromagnetic state. Owing to

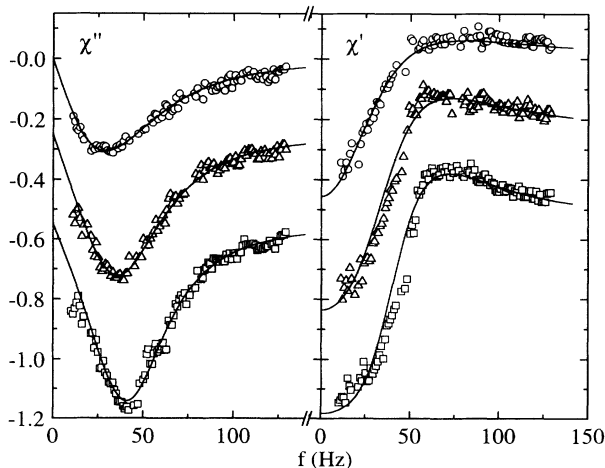


FIG. 1. NMR absorption χ'' and dispersion χ' curves (in dimensionless SI units) of the nuclear spin system in silver at $T < 0$, measured in zero field at reduced entropies $S/R \ln 2$ equal to 0.87 (○), 0.80 (△), and 0.73 (□), which correspond to polarizations $p = -0.42$, -0.51 , and -0.59 in the paramagnetic state, respectively. The zeros for the lower curves have been shifted downwards by 0.25 and 0.55 in both frames.

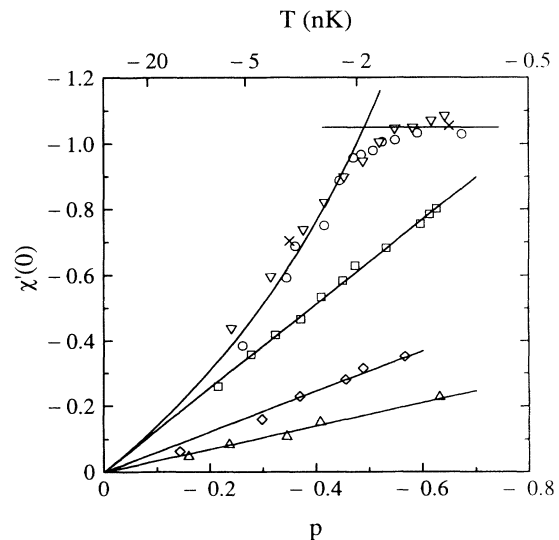


FIG. 2. Static susceptibility $\chi'(0)$ vs polarization p of silver nuclear spins at $T < 0$, measured in a magnetic field B_y of 0 (○), $5 \mu\text{T}$ (▽), $20 \mu\text{T}$ (□), $50 \mu\text{T}$ (◇), and $100 \mu\text{T}$ (△), and at $B_z = 5 \mu\text{T}$ (×). The fitted curves are discussed in the text. The scale on top gives estimated temperatures based on the formula [9] $1/|p| - 1 = 0.55|T|$ (in nK), which applies only at $B = 0$; values to the right of -2 nK must be considered tentative.

the rounding of $\chi(p)$, we estimate conservatively, in zero field and at $5 \mu\text{T}$, for the critical polarization $p_c = 0.49 \pm 0.05$, which corresponds to $S_c/\mathcal{R}\ln 2 = 0.82 \pm 0.035$. This critical entropy is quite large when compared with the values for antiferromagnetic ordering, $S_c/\mathcal{R}\ln 4 = 0.48-0.61$ and $S_c/\mathcal{R}\ln 2 = 0.53$, in copper [1] and silver [2], respectively. By employing the linear relationship between the temperature and inverse polarization, $1/|p| - 1 = 0.55|T|$ (in nK), determined in earlier experiments [9], we obtain $T_c = -1.9 \pm 0.4$ nK; this value may have a systematic error of 20%, owing to the uncertainty of the relationship between p and T at negative temperatures.

We also tried to determine T_c directly from the weighted average (first moment) of our NMR data, which display a clear minimum (see Fig. 3) at $p = 0.3$; this suggests a lower critical polarization than the saturation of χ . We think, however, that the analysis based on Fig. 2 is more reliable since the behavior of the NMR frequencies upon ordering is not very well understood.

According to the mean-field theory, $T_c = \theta = -5$ nK in silver; this is clearly larger than the observed value. Calculations [11] on the spin- $\frac{1}{2}$ Heisenberg model in an fcc lattice yield $T_c = 0.67\theta = -3.4$ nK, which exceeds our result by 80%; the computed value does not change much even if the small next-nearest-neighbor interaction is taken into account [12]. In contrast, the critical entropy according to the Heisenberg model, $S_c = 0.66\mathcal{R}\ln 2$, is clearly lower than our experimental value. This is reasonable since the long-range dipolar interaction acts ferromagnetically at negative temperatures owing to domain formation, which increases S_c in silver.

Monte Carlo calculations [13] predict $T_c = -1.7$ nK, which is close to our measured result. However, the computed critical entropy $S_c = 0.93\mathcal{R}\ln 2$ deviates substantially from the experimental value, which indicates that the

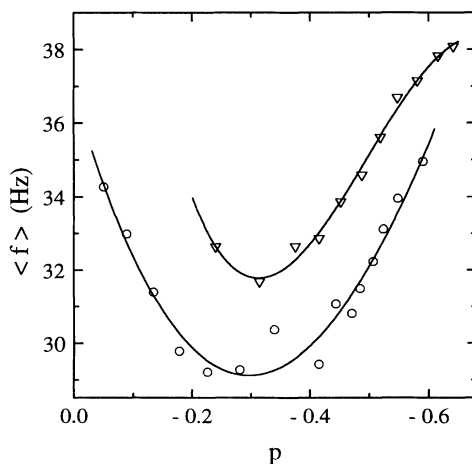


FIG. 3. First moment $\langle f \rangle$ of the NMR line shapes as a function of p , measured in zero field (O) and at $B_y = 5 \mu\text{T}$ (∇). The curves are just to guide the eyes.

good agreement between the theoretical and experimental data on T_c may be fortuitous.

The saturation of susceptibility to $\chi_{\text{sat}} \cong -1$ in the ordered state can be explained only by the formation of domains, since otherwise the susceptibility would diverge at T_c . Instead of needles, as at $T > 0$, plate-shaped domains are expected [4]. According to mean-field calculations [13], a ferromagnetic state with broken plate-shaped domains yields $\chi_{\text{sat}} = -1/(1 - D_M)$; here D_M is the demagnetization factor along the spontaneous magnetization \mathbf{M} . This is in agreement with our results at $B = 0$ and $B_z = 5 \mu\text{T}$. In a small transverse field, however, \mathbf{M} is perpendicular to the plates and a much larger χ should result, but it was not observed at $B_y = 0-10 \mu\text{T}$. This suggests the presence of a single-domain state which can be stable in a transverse field. The mean-field theory [14] then yields $\chi_{\text{sat}} = -1/(D_y - D_z) = -1.33$, which is fairly close to the experimental value $\chi_{\text{sat}} = -1.05$. Moreover, Monte Carlo simulations [13] have confirmed the mean-field result in the ideal case when $D_y - D_z = 1$.

At higher fields, $\chi'(0)$ is directly proportional to p (see Fig. 2), i.e., the behavior is paramagnetic. The saturation of susceptibility was lost in the $\chi(t)$ sweeps already around $10 \mu\text{T}$ and a reliable determination of the transition point became impossible. On the basis of the detected transitions at 0 and $5 \mu\text{T}$ (see Fig. 2), we have constructed a schematic B vs $S/\mathcal{R}\ln 2$ phase diagram for silver which is depicted in Fig. 4. We estimate $B_c = -\mu_0 M_{\text{sat}}/\chi_{\text{sat}}(T=0) \cong 40 \mu\text{T}$ at zero temperature; this value has been used when drawing the dashed transition curve for the ferromagnetic phase.

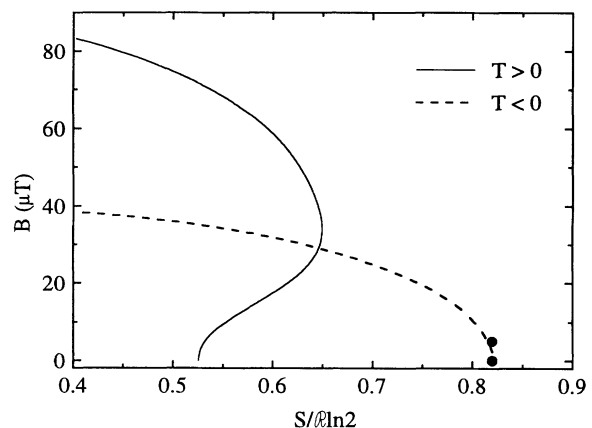


FIG. 4. Phase diagram in the B vs $S/\mathcal{R}\ln 2$ plane for the nuclear spins in silver metal at negative absolute temperatures. Solid circles represent our experimental data, obtained from Fig. 2, and the dashed curve displays a theoretical phase boundary between the ferromagnetic (at left) and paramagnetic regions. The shape of this curve is based on the mean-field theory [11] with the assumption of a linear relationship between S and T . The antiferromagnetic phase transition curve at $T > 0$ [2], marked by the solid line, is included for comparison.

We searched for hysteresis in $M(B)$ in the ordered state by measuring χ' at the fixed frequency of 10 Hz while sweeping the transverse magnetic field between $\pm 30 \mu\text{T}$. The adiabatic susceptibility $\chi'(10 \text{ Hz})$ displayed a small, 5% asymmetry in amplitude with respect to zero field, but less than $0.5 \mu\text{T}$ of hysteresis between opposite field sweeps. Since the hysteresis was so small, we prefer to assign the observed asymmetry in $\chi'(10 \text{ Hz})$ to small changes in the phase of the signal during the field sweep while keeping a constant phase setting in the lock-in amplifier.

In summary, we have made the first observation of a ferromagnetic state in a metallic nuclear spin system at $T < 0$. Comparison of the saturation values of susceptibility with the mean-field theory and Monte Carlo calculations [13] indicate that in fields parallel to the sample plates there is a multidomain state in silver, while in a transverse field a single-domain structure is preferred. The hysteresis in $M(B)$ was found to be small, less than $0.5 \mu\text{T}$, which points to a ferromagnetic system without anisotropy. The measured critical entropy, $S_c = 0.82\mathcal{R} \times \ln 2$, is larger than the value for the Heisenberg model, $S_c = 0.66\mathcal{R} \ln 2$, which indicates that, even though the Ruderman-Kittel exchange is dominating, the dipolar interaction substantially helps in the ordering process at $T < 0$; this leads to a ferromagnetic phase diagram which differs substantially from that of the antiferromagnetic state at $T > 0$.

Useful interaction with A. Oja and H. Vieriö on theoretical issues is gratefully acknowledged. This work was supported by the Academy of Finland.

- [1] M. T. Huiku and M. T. Lopenen, Phys. Rev. Lett. **49**, 1288 (1982); A. J. Annala, K. N. Clausen, P.-A. Lindgård, O. V. Lounasmaa, A. S. Oja, K. Siemensmeyer, M. Steiner, J. T. Tuoriniemi, and H. Weinfurter, Phys. Rev. Lett. **64**, 1421 (1990).
- [2] P. J. Hakonen, S. Yin, and K. K. Nummila, Europhys. Lett. **15**, 677 (1991).
- [3] For a recent review, see P. J. Hakonen, O. V. Lounasmaa, and A. S. Oja, J. Magn. Magn. Mater. (to be published).
- [4] See, e.g., A. Abragam and M. Goldman, *Nuclear Magnetism: Order and Disorder* (Clarendon, Oxford, 1982).
- [5] P. Bonamour, V. Bouffard, C. Fermon, M. Goldman, J. F. Jacquinot, and G. Saux, Phys. Rev. Lett. **66**, 2810 (1991).
- [6] P. J. Hakonen, S. Yin, and O. V. Lounasmaa, Phys. Rev. Lett. **64**, 2707 (1990).
- [7] J. Pointreud and J. M. Winter, J. Phys. Chem. Solids **25**, 123 (1964).
- [8] A. S. Oja, A. J. Annala, and Y. Takano, Phys. Rev. Lett. **65**, 1921 (1990).
- [9] P. J. Hakonen and S. Yin, J. Low Temp. Phys. (to be published).
- [10] G. J. Ehnholm, J. P. Ekström, J. F. Jacquinot, M. T. Lopenen, O. V. Lounasmaa, and J. K. Soini, J. Low Temp. Phys. **39**, 417 (1980).
- [11] See, e.g., L. J. de Jongh and A. R. Miedema, Adv. Phys. **23**, 1 (1974).
- [12] This has been reviewed briefly, e.g., by R. H. Swendsen, Phys. Rev. Lett. **32**, 1439 (1974).
- [13] H. E. Vieriö and A. S. Oja, J. Magn. Magn. Mater. (to be published).
- [14] H. E. Vieriö and A. S. Oja (private communication).